Microchimica Acta (2018) 185: 142
https://doi.org/10.1007/s00604-018-2682-0

ORIGINAL PAPER

Reusable resistive aptasensor for Pb(II) based on the Pb(II)-induced despiralization of a DNA duplex and formation of a G-quadruplex

Hui Wang[1] · Yang Liu[2] · Gang Liu[1]

Received: 7 November 2017 / Accepted: 15 January 2018 / Published online: 29 January 2018

Abstract

The article describes a reusable biosensor for Pb(II) ions. A duplex DNA with a terminal amino group and containing a G-quadruplex (G4) aptamer was covalently conjugated to single walled carbon nanotubes on a field effect transistor (FET). The detection scheme is based on the despiralization of the DNA duplex because Pb(II) can induce the G4 aptamer to form a stabilizing G4/Pb(II) complex. This structural change affects the electrical conductivity of SWNTs which serves as the analytical signal. The biosensor was characterized via scanning electron microscopy, Raman, UV-vis, and voltage-current profiles. Under optimized conditions, the relative resistance at 0.02 V increases linearly with the logarithm of the Pb(II) concentration in the range from 1 ng·L^{-1} to 100 μg·L^{-1}, and the limit of detection is 0.39 ng·L^{-1}. Compared to other sensors, this oner demonstrates superior simplicity, sensitivity, and selectivity even in mixtures of heavy metal ions. It was applied to the determination of Pb(II) in (spiked) water and soil samples and gave good results.

Keywords Field effect transistor · Electroanalysis · Single walled carbon nanotubes · Lead ion · DNA · Heavy metal · Nanomaterial-based sensing

Introduction

Lead is one of the most toxic contaminants because its bioaccumulation in the food chain is an ongoing hazard to human health. Lead pollution originates primarily from batteries, building construction, mining, industrial use, waste incineration, coal and gasoline burning [1–3]. Based on a survey, over 300 million tons of lead has been mined to date, and are circulating in soil and groundwater [4]. Lead in the human body is derived from contaminated air, water, soil, and food through inhalation and ingestion [5, 6]. Once lead ions are introduced into the human body, they will be rapidly absorbed through the digestive system and into the bloodstream. Lead ions may bind to the sulfhydryl groups existed of various enzymes [7, 8]. Besides, it may also mimick and displace other essential metal ions such as calcium, iron, and zinc, which are essential elements for plants and humans as catalytic components of proteins and enzymes [9]. High content of lead in human body will affect the normal functioning of organs with symptoms including nephropathy [10], colic-like abdominal pains [11], and possibly weakness in the fingers, wrists, or ankles [12]. Therefore, monitoring the content of lead in food and environment is important for decreasing lead intake and environmental pollution.

There is a variety of analytical methods for lead ion determination including flame atomic absorption spectrometry (FAAS) [13], inductively-coupled-plasma mass spectrometry(ICP-MS) [14], inductively coupled plasma

Hui Wang and Gang Liu contributed equally to this work.

Electronic supplementary material The online version of this article (https://doi.org/10.1007/s00604-018-2682-0) contains supplementary material, which is available to authorized users.

✉ Gang Liu
pac@cau.edu.cn

Hui Wang
wanghui_lunwen@163.com

[1] Present address: Key Laboratory of Modern Precision Agriculture System Integration Research, Ministry of Education and Key Laboratory of Agricultural Information Acquisition Technology, Ministry of Agriculture China Agricultural University, Beijing 100083, People's Republic of China

[2] School of Electronic and Information Engineering, Xi'an Jiaotong University, Xi'an 710049, People's Republic of China

atomic emission spectrometry (ICP-AES) [15], X-ray fluorescence spectrometry [16], and atomic fluorescence spectrometry (AFS) [17]. Despite high selectivity and sensitivity, these methods require expensive and complicated instruments, complex operation and sample pretreatment processes that limit their applications for on-site monitoring [18]. Hence, rapid, sensitive and low-cost methods are needed for the determination of heavy metal ions in situ.

DNA or DNAzyme can specifically bind heavy metal ions, which have shown great promise for qualitative and quantity detection. Many researchers have reported plenty of sensors for the metal ions detection, including Pb(II), Zn(II), Hg(II), Cu(II), Ca(II), Ag(I) and K(I). As for Pb(II) detection, Kevin W. Plaxco et al. [19] designed an electrochemical sensor based on lead-dependent changes in the conformational state of a surface-immobilized, methylene-blue modified DNAzyme assembly for the detection of parts-per-billion lead. Chung [20] selected highly Pb(II)-specific DNA-aptamer sequences based on CD spectroscopy of G-rich DNA sequences and Hg(II)-specific T-rich DNA sequences and immobilized them on gold nanoparticles for the simultaneous detection of Pb(II) and Hg(II) in human serum. DNAzyme based on metal ion cleaved RNA is sensitive, but the structure will be destroyed that lead to high-cost and hard to reuse. In contrast with DNAzyme, aptamer as a single-stranded DNA has high affinity and selectivity to bind with targets, which only change the structure that offers a huge potential to design a reusable sensor.

In this paper, a reusable biosensor using a G-quadruplex aptamer (G4-DNA) and complementary single-stranded DNA(CS-DNA) with amino group had been developed, which was immobilized on SWNTs-modified FET through a peptide bond. The number of bases in the duplex DNA was optimized so that Pb(II) can drive the double-stranded DNA to despiralize G4-DNA and CS-DNA, and induce the aptamer to form a stabilizing G4/Pb(II) complex at normal temperature. This structural change can affect the electrical conductivity of SWNTs, which were employed to quantify the low-concentration of Pb(II). After each detection, the single CS-DNA were rebind with G4-DNA, which can make the biosensor for reuse.

Materials and methods

Chemicals and materials

Single-walled carbon nanotube solution (0.01 mg·mL^{-1}, 95% semiconducting) was offered by Nano-Integris Inc. (USA, https://www.nanointegris.com/). 1-Pyrenebutanoic acid succinimidyl ester (PBASE) was bought from Invitrogen Inc. 3-Aminopropyltriethoxysilane (APTES, 99%) and ethanolamine (EA, 99%) were bought from Acros Organics (USA, https://www.fishersci.com/). Potassium hydrogen phosphate, monopotassium phosphate and 6-mercapto-1-hexanol (MCH, 97%) were purchased from Sigma Aldrich (USA, https://www.sigmaaldrich.com/). Tween 20 was obtained from Bio-Rad. Standard solutions of all metals (Pb(II), Na(I), K(I), Ca(II), Hg(II), Cd(II), Zn(II), Cu(II), Fe(III), and Cr(III)) were provided by National Standard Reference Materials Center (China, http://www.bzwz.com/). Double distilled water was used throughout. The rest of chemicals not mentioned here were of analytical reagent grade and were used without further purification. Tris-HCl buffer (10 mmol·L^{-1}, pH 7.4) was selected as the supporting electrolyte. Ultra-pure grade water from a Millipore Milli-Q system was used through this experiment.

Ultrapure oligonucleotides, G-quadruplex aptamer (G4-DNA), complementary single-stranded DNA(CS-DNA), no-specific DNA(NS-DNA) were synthesized using standard solid phase techniques by Sangon Biotechnology Co., Ltd. (Shanghai, China).

GS4-DNA: 5′-NH_2-GGGTG GGTGGGTGGGT-3′	G4-DNA: 5′- TGGGTGGGTGGG TGGG-3′
CS0-DNA: 5′-ACCCACCCAC CCACCC-3′	CS-DNA: 5′- NH_2 -CCCACCCACCCTT TTT −3′
CS1-DNA: 5′-TTTTACCCACCC ACCC-3′	NS-DNA: 5′- AAAAATGGGTG TGA-3′
CS2-DNA: 5′-TTTTTCCCACC CACCC-3′	
CS3-DNA: 5′-TTTTTTCCACCC ACCC-3′	
CS4-DNA: 5′-TTTTTTTCACC CACCC-3′	
CS5-DNA: 5′-TTTTTTTTACCC ACCC-3′	

Apparatus

The current-voltage (I-V) characteristics of the device were recorded using a semiconductor parameter analyzer, Keithley 2636. For I-V measurement, the current between the drain and the source was measured using linear weep voltammetry ramping the drain-source voltage(V_{DS}) from −0.1 V to +0.1 V with $V_G = 0$ V. SEM images were obtained by a Zeiss Leo SUPRA 55 with beam energy of 10 kV. Raman spectra were measured through Dilor XY Laser Raman with imaging microscope (532 nm Diode and Ar ion lasers). UV-vis spectra were recorded on a Beckman DU800 UV/Vis spectrophotometer (Beckman Coulter, Inc. USA) and step scan (0.5 cm^{-1} resolution).

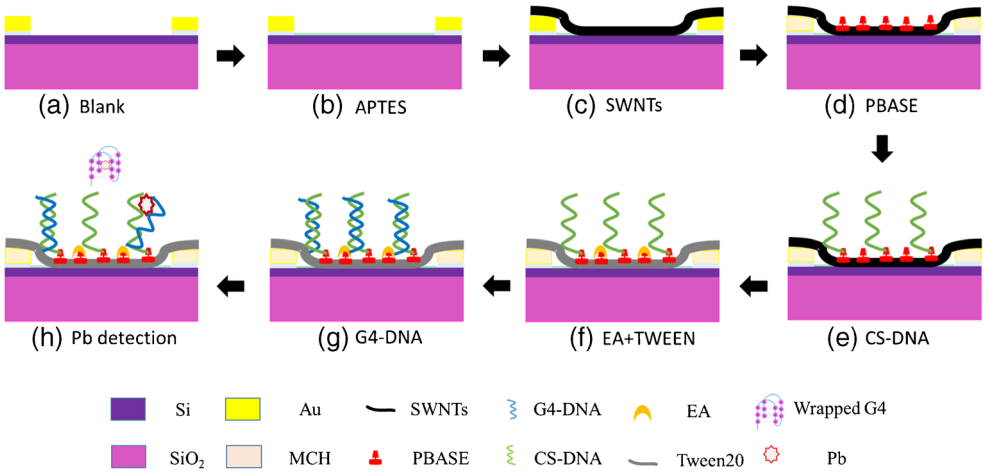

Fig. 1 A schematic of the device fabrication and sensing protocol

Fabrication of biosensor

The biosensor was fabricated using an interdigital electrode in Fig.S1(A), which has 10 pairs of interdigitated finger with a 200 μm in length and a 5 μm in width. The gap between two adjacent interdigitated fingers was 3 μm. This electrode was made by depositing a 20 nm Cr layer and an180 nm Au layer on a high doped p-type silicon substrate with 100 nm SiO_2 dielectric layer, and written through standard lithographic patterning.

The interdigital electrode was modified in following steps. First, it was cleaned with acetone, isopropanol, and ammonium hydroxide, respectively. The cleaned chip was immersed in 0.5 mL 99% APTES for 60 min, and then washed with sufficient Milli-Q water. After that, the chip was covered by 10 μL SWNTs suspension and incubated with high humidity conditions for 60 min, followed by washing the SWNTs residual and annealing in air at 250 °C. The morphologic structure of SWNTs on the electrode is shown in Fig.S1(B). The gold surface was blocked with 10 mmol·L^{-1} MCH solution prepared in ethyl alcohol to prevent any non-specific binding of proteins. Next, the SWNTs' area was covered by 100 μL 6 mmol·L^{-1} PBASE prepared in DMF through noncovalent bond between pyrene and SWNTs for 60 min. The PBASE-modified SWNTs were incubated with 10 μL 100 nmol·L^{-1} CS-DNA overnight under high humidity at 4 °C. The CS-DNA was immobilized covalently via an amide bond between the amino group at the 5′ end and the ester groups of PBASE. The device was further treated with 50 μL 0.1 mmol·L^{-1} EA for 60 min to block excess ester groups, and 50 μL 0.1% Tween 20 for 60 min to prevent non-specific binding to SWNTs. Finally, the CS-DNA captured on the SWNT surface was hybridized with G4-DNA by incubating with 10 μL 100 nmol·L^{-1} G4-DNA in PB for 120 min at room temperature to form a DNA duplex. After each measurement, the used biosensor was washed with Milli-Q water for several times, and incubated with 10 μL 100 nmol·L^{-1} G4-DNA for 120 min (Fig. 1).

Sensing protocol

To determinate the content of Pb(II), the biosensor was covered with 50 μL Tris-HCl buffer, and measured the current (I_0) at 0.02 V. Subsequently, the biosensor was incubated with 50 μL Pb(II) solution for 30 min at room temperature, and then rinsed with Tris-HCl buffer three times to remove the Pb(II) residues. Next, the washed device was covered with 50 μL Tris-HCl buffer, and measured the current (I) at 0.02 V again. The resistance was calculated using R = U/I. All measurements were repeated for a minimum of three electrodes to obtain statistically reliable results.

The relative change of resistance was defined as follow:

$$\text{Relative resistance} = (R_0 - R)/R_0 \times 100\%$$

Where R_0 was the initial resistance value and R is the resistance after explored to Pb(II) solution.

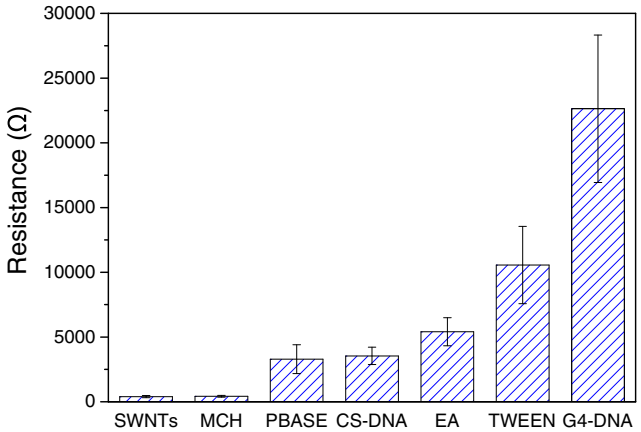

Fig. 2 Changes in resistance after FET functionalized with SWNTs, MCH, PBASE, CS-DNA, EA, Tween20 and G4-DNA at 0.02 V. Each data point is an average of measurements from 5 independent biosensors

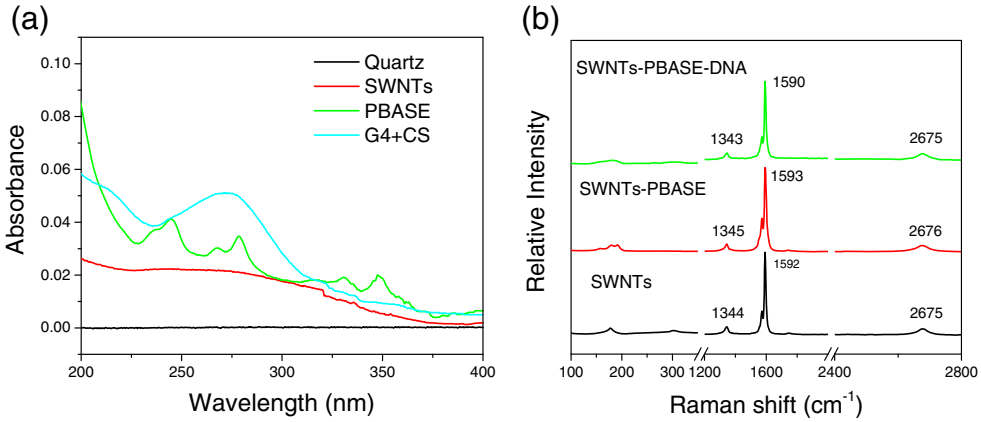

Fig. 3 **a** UV-vis absorption spectra of quartz (Black), SWNTs (Red), PBASE (Green), and G4+ CS-DNA (Blue); (**b**) Raman spectra of SWNTs (Black), PBASE/SWNTs (Red), and CS+ G4-DNA/ PBASE/SWNTs (Green)

Results and discussion

Choice of materials

G4-DNA as molecular recognition probe exhibits a specific binding affinity for Pb(II), which can be induced Pb(II) to form an ultrahigh stable structure [21]. Complementary DNA strand (CS-DAN) of G4-DNA was immobilized onto SWNTs-FET. To reduce the cost and simplify the experiment, CS-DNA and G4-DNA with amino group were employed during the experiment optimization process.

Characterization of DNA-SWNTs

The electrical properties of different materials were functionalized on SWNTs-FET, and measuring current-voltage (I-V) were characterized to confirm. As shown in Figure S2, I-V curves were observed over a range of −0.1 V to +0.1. The currents of modified FET device decrease markedly after following each treatment step, indicating that MCH, PBASE, CS-DNA, EA, Tween 20 and G4-DNA have been functionalized on the device. The changes in the resistance were exhibited in Fig. 2. After MCH modification, the resistance was almost no change, ascribing that MCH only bind with gold through Au-S bonds. When the device was functionalized with PBASE, amine labeled CS-DNA, EA, Tween 20 and G4-DNA, the resistance increased significantly. The reason is mainly that electron donation from PBASE, amine labeled G4-DNA, EA, Tween 20 and CS-DNA resulted in a decrease of the charge carrier concentration of the p-type SWNTs and electron scattering from these molecules.

To further confirm the functionalization of DNA-SWNTs, the silicon substrate was replaced with a quartz plate due to its superior optical characteristics. The UV-vis measurements shows in Fig. 3. After the quartz was modified with SWNTs, the absorption in the range of 200–300 nm improved as shown by the gentle peak, which was attributed to the absorption peak of SWNTs at 260 nm [22]. The curve of SWNT-PBASE revealed three weak peaks, indicating SWNTs had attached with pyrene through the π interaction between the pyrene ring and SWNT sheet [23, 24]. While PBASE-SWNTs functionalized with CS-DNA and G4-DNA, they generated a composite effect that UV-vis spectra peak at 275 nm. Due to the UV-vis absorption peak of DNA at 260 nm, the two weak peaks of PBASE were overlapped with DNA's to form a large peak [25]. Raman spectroscopy is a powerful method to investigate changes in the properties of carbon nanomaterials [26]. The Raman spectra with 514 nm laser excitation from 100 to 2800 cm^{-1} are shown in Fig. 4.

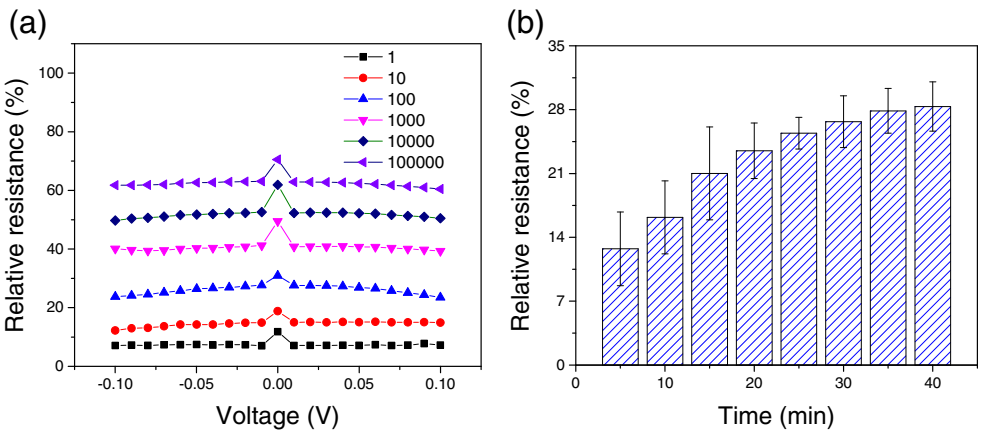

Fig. 4 **a** The change of relative resistance at the V_{DS} ranging from −0.1 V to +0.1 V for the detection of different Pb(II) concentrations(1, 10, 100, 1000, 10,000 and 100,000 ng·L^{-1}). **b** The relative resistance for 1000 ng·L^{-1} Pb(II) detection effected by different incubation times(5, 10, 15, 20, 25,30, 35 and 40 min). Each data point is an average of measurements from 5 independent biosensors

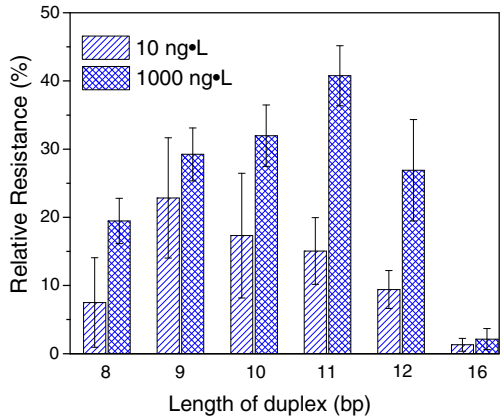

Fig. 5 The effect of length of duplex base pairs in the duplex with the concentration of 10 and 1000 ng·L^{-1} Pb(II).Each data point is an average of measurements from 5 independent biosensors

While SWNTs was treated with PBASE, D, G and 2D peaks were shifted to the right slightly, indicating that PBASE attached to the SWNTs surface [27]. After DNA had immobilized on PBASE-SWNTs, the relative intensity of all peaks decreased considerably, which were mainly ascribed that DNA existed on PBASE-SWNTs' surface.

Optimization

The parameters of incubation time and the voltage between source and drain were optimized. In order to simplify the experimental process, we chosen the GS4-DNA with the amino and CS-DNA for the optimizing research. Fig. S2(A) shows the voltage-current in the range from −0.1 V to +0.1 V, which presents a nonlinear, and the resistance decreased by increasing voltage. However, the relative resistances calculated with formula were a constant in the range from −0.01 V to −0.01 V and 0.01 to +0.01 V in Fig. 4a, which indicated all the voltage are the same. Therefore, +0.02 V was chosen for the following experiments. The dynamic change of resistance results in the incubation time ranging from 0 to 40 min in Fig. 4b. The device was dipped into the lead standard solution of 100 ng·L^{-1}, and measured the voltage-current for every 5 min. It was found that the resistance decreases dramatically at the beginning of 30 min, indicating that Pb(II) made the two DNA strands separate and induced aptamer switch from hairpin to G-quadruplex. Twenty minutes later, the resistance was found to decrease only slightly or level off possibly because the Pb(II) bond with G-quadruplex reduced the concentration in solution. For these reasons, the incubation time of 30 min was selected.

The number of base pairs in the duplex can influence the efficiency of Pb(II)-induced structural conversion from the duplex to G-quadruplex. To find out the optimal base pairs, a different number of base pairs were tested. Figure 1h shows that the duplex with different base pairs exhibited a distinct response to the addition of Pb(II). Figure 5 illustrates the relationship between a different number of base pairs in the DNA duplex and response intensity for certain Pb(II) concentrations. When the 16 bases of G4-DNA bond with the complementary strand DNA, no signals found after the biosensor was exposed to 1 and 1000 ng·L^{-1} Pb(II), indicating no structural conversion induced by Pb(II). This is mainly because the melt temperature of the formed duplex DNA reaches 61 °C so that it was stable at room temperature. As the base pairs of the duplex decreased gradually, the Pb(II)-induced structural conversion was more and more easily achieved at room temperature. However, if the number of base pairs was lower, the response was lower. This was ascribed to smaller number of base pairs lacking enough energy to keep stable. For the reasons discussed above, 11 base pairs in DNA was selected.

The effect of the base type of aptamer on the performance of the biosensor with the two Pb(II) concentrations (100 ng·L^{-1} and 10,000 ng·L^{-1}) in Fig. S5. When G4-DNA is replaced by NS-DNA, the relative resistances were no change in presence of different Pb(II) concentrations. Therefore, it indicated that G4-DNA can bind with Pb(II) effectively (Fig. 6).

The biosensor was exposed to standard solutions containing different concentrations of Pb(II) under the

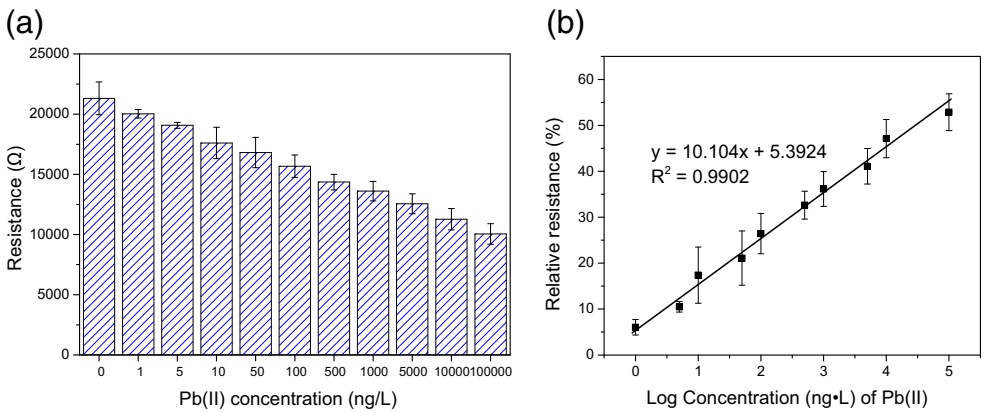

Fig. 6 **a** The resistances of biosensor for the detection of different Pb(II) concentrations (0, 1, 5, 10, 50, 100, 500, 1000, 5000, 10,000 and 100,000 ng·L^{-1}). **b** Calibration curve for Pb(II) detection. Each data point is an average of measurements from 5 independent biosensors

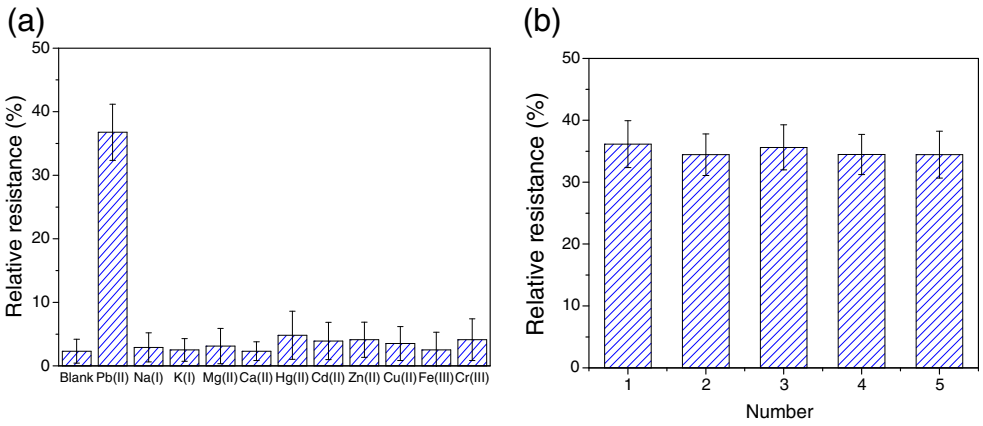

Fig. 7 **a** Selectivity of the biosensor measured 1000 ng·L^{-1} Pb(II) and several co-existing ions (100,000 ng·L^{-1}) in absence of Pb(II) **b** Reproducibility of the biosensor measured 1000 ng·L^{-1} Pb(II) after CS-DNA/SWNTs/FET re-bond with G4-DNA. Each data point is an average of measurements from 5 independent biosensors

optimum conditions, and shows the relationship between the resistances and Pb(II) concentrations. The resistance decreased with the increasing concentration of Pb(II) in Fig. 7a, which indicated that the duplex gradually converts into the G4 structure by Pb(II). It was clear that relative resistance increases linearly with the logarithm of Pb(II) concentration variation from 1 ng·L^{-1} to 100,000 ng·L^{-1}. The linear regression equation was $y = 10.104\ log[Pb(II)] + 5.8656\ (R^2 = 0.9902)$, and the detection limit (S/N = 3) was found to be 0.39 ng·L^{-1}. We found the sensitivity of CS-DNA/SWNTs/FET was lower than the G4-DNA/SWNTs/FET, but the CS-DNA/SWNTs/FET can realize multiple use, which was selected for further application. As shown in Table 1, some parameters of different published sensors for Pb(II) determination were listed. Compared to other sensors [30–35], the proposed biosensor had a wide linear detection range and low detection limit for Pb(II).

Interference

Metal ions in real samples usually interfere with the detection of Pb(II). To evaluate the selectivity, other common interfering 9 metal ions (Na(I), K(I), Ca(II), Hg(II), Cd(II), Zn(II), Cu(II), Fe(III), and Cr(III)) coexist with Pb(II) were evaluated. Figure 7a shows the relative resistance of the biosensor against 1000 ng·L^{-1} Pb(II) before and after adding other metal ions (100,000 ng·L^{-1}). We found that K(I) and Cr(III) can cause a slight change in the relative resistance, and the rest signals were almost no change. All the relative errors were no more than 4, which demonstrated that the biosensor had an excellent selectivity toward Pb(II).

Reproducibility

To investiage the reproducibility, the same biosensors were measured the 1000 ng·L^{-1} Pb(II) stardard solution, and re-bond with G4-DNA for 120 min after each detection. Figure 7b shows the first five results that indicated the biosensors had good reproducibility because the relative resistance and standard deviation of five times determination were almost unchange.

Analysis of real sample

To evaluate the practical application of the prepared biosensor, the real samples (lake water, and the soil from lake and field) were applied in this study. The samples of lake water

Table 1 Comparison of the prepared biosensor for Pd(II) detection with other published sensors

Sensor	Method	Liner ranges (mol·L^{-1})	Determination limits (mol·L^{-1})	Reference
GCE/Amino-AT	ASDPV	4.0×10^{-12}~4.0×10^{-11}	0.88×10^{-12}	[28]
nsBiFE	ASV	1.0×10^{-8}~5.0×10^{-7}	1.0×10^{-9}	[29]
NG/GCE	DPSV	1.0×10^{-8}~9.0×10^{-6}	5.0×10^{-9}	[30]
AuNPs-Apt-CS-GCE	DPV	0.7×10^{-9}~1.0×10^{-7}	1.0×10^{-12}	[31]
DNAzyme/OMC-GNPs/GCE	EIS	5.0×10^{-10}~5.0×10^{-5}	2.0×10^{-12}	[32]
DNAzyme/GR/FET	FET	1.8×10^{-10}~1.2×10^{-7}	2.4×10^{-12}	[33]
AuNPs/SPCE	SWASV	4.8×10^{-8}~4.8×10^{-7}	1.0×10^{-11}	[34]
CS-DNA/SWNTs/FET	IV	4.8×10^{-12}~ 4.8×10^{-7}	1.56×10^{-12}	This work

Table 2 Lead ion concentration in environmental sample determined by proposed method and FAAS

Sample	Adding Pd(II) ($\mu g \cdot L^{-1}$)	Biosensor Detection concentration[a] ($\mu g \cdot L^{-1}$)	FAAS method Detection concentration ($\mu g \cdot L^{-1}$)	Relative error (%)
Lake water 1	–	0.78 ± 0.18	0.74 ± 0.04	4.48
	5	5.93 ± 0.35	–	1.65
Lake water 2	–	1.34 ± 0.23	1.41 ± 0.06	3.92
	5	6.85 ± 0.52	–	2.60
Soil 1	–	16.59 ± 0.39	17.31 ± 0.35	4.16
	10	26.48 ± 0.54	–	3.10
Soil 2	–	22.61 ± 0.67	21.57 ± 0.39	4.82
	10	32.82 ± 0.86	–	3.96

[a] Means of three determinations

and tap water were collected from different sites along the lake or river banks, and then filtered through a 0.22 μm membrane to remove insoluble substances. Soil samples were collected from a local field in Beijing, and pretreated using the following steps [35]. First, soil samples were heated to 200 °C for 30 min, and then ground into small particles. 1 g soil and 20 mL of 0.5 $mol \cdot L^{-1}$ hydrochloric acid were mixed, and sonicated for 60 min at room temperature. After these steps, the mixture solution was centrifuged and filtered by a 0.22 μm membrane. Finally, all filtered solutions were adjusted the pH using Tris-HCl.

These samples were measured by the biosensor for three parallel times, and the results were listed in Table 2. To estimate the accuracy of the detection values, the standard addition method and flame atomic absorption spectrometry were used to detect further. For comparing the results of the proposed biosensor with those of FAAS, the results shown quite near between these two methods and the relative errors were below 5%. We also used t-test to analyze these results of two methods, which can get $P = 0.978 > 0.05$. It can be concluded that there was no significant difference between the results obtained by the two methods, indicating that the proposed biosensor was accurate and reproducible.

Conclusion

In this study, an innovative SWNTs-based biosensor based on Pb(II)-driven a DNA duplex to form G4-DNA/Pb(II) complex was fabricated for the purpose of Pb(II) detection. The biosensor for the detection of Pb(II) has excellent characeristics, including high sensitivity, reusablitiy, and selectivity. Compared with methods, the proposed method prossessed unique features, such as cost effectiveness, easy-to-use, low reagent volumes. But it still existed some deficiencies. The detection accuracy of biosensor is vulnerable to the environment, especially temperature.

Acknowledgements This work was supported by Chinese National Natural Science Foundation (No. 31671578), National High Technology Research and Development Program of China (No.2013AA102302), the Fundamental Research Funds for the Central Universities (No. 2016 XD001) and the Shandong Provincial Natural Science Foundation of China (No. ZR2015CM016).

Compliance with ethical standards The authors declare no competing financial interests.

References

1. Haefliger P, Mathieu-Nolf M, Lociciro S, Ndiaye C, Coly M, Diouf A, Faye AL, Sow A, Tempowski J, Pronczuk J (2009) Mass lead intoxication from informal used lead-acid battery recycling in Dakar, Senegal. Environ Health Perspect 117:1535
2. Chen K, Huang L, Yan BZ, Li HB, Sun H, Bi J (2014) Effect of lead pollution control on environmental and childhood blood lead level in Nantong, China: an interventional study. Environ Sci Technol 48: 12930–12936
3. Walraven N, Bakker M, van Os B, Klaver G, Middelburg JJ, Davies G (2016) Pollution and oral bioaccessibility of Pb in soils of villages and cities with a long habitation history. Int J Env Res Pub He 13
4. He QW, Miller EW, Wong AP, Chang CJ (2006) A selective fluorescent sensor for detecting lead in living cells. J Am Chem Soc 128:9316–9317
5. Li T, Shi LL, Wang EK, Dong SJ (2009) Silver-ion-mediated DNAzyme switch for the ultrasensitive and selective colorimetric detection of aqueous Ag+ and cysteine. Chem-Eur J 15:3347–3350
6. Yu Y, Li YX, Li B, Shen ZY, Stenstrom MK (2016) Metal enrichment and lead isotope analysis for source apportionment in the urban dust and rural surface soil. Environ Pollut 216:764–772
7. Ma W (1996) Lead in mammals, environmental contaminants in wildlife: interpreting tissue concentrations. CRC Press, Boca Raton, pp 281–296
8. Pareja-Carrera J, Mateo R, Rodríguez-Estival J (2014) Lead (Pb) in sheep exposed to mining pollution: implications for animal and human health. Ecotox Environ Safe 108:210–216

9. Gourlaouen C, Parisel O (2007) Is an electronic shield at the molecular origin of lead poisoning? A computational modeling experiment. Angew Chem Ed 46:553–556
10. Bhattacharjee T, Bhattacharjee S, Choudhuri D (2016) Hepatotoxic and nephrotoxic effects of chronic low dose exposure to a mixture of heavy metals–lead, cadmium and arsenic. Int J Pharma Chem Biol Sci 6:39–47
11. Araujo J, Beelen A, Lewis L, Robinson G, DeLaurier C, Carbajal M, Ericsson B, Chin Y, Hipkins K, Kales S (2004) Lead poisoning associated with Ayurvedic medications—five states, 2000-2003, MMWR- Morbidand mortal w. 53: 582
12. Kernich CA (2001) Peripheral neuropathy. Neurologist 7:315–316
13. Duran C, Gundogdu A, Bulut VN, Soylak M, Elci L, Senturk HB, Tufekci M (2007) Solid-phase extraction of Mn(II), Co(II), Ni(II), Cu(II), Cd(II) and Pb(II) ions from environmental samples by flame atomic absorption spectrometry (FAAS). J Hazard Mater 146:347–355
14. Sorbo A, Turco AC, Di Gregorio M, Ciaralli L (2014) Development and validation of an analytical method for the determination of arsenic, cadmium and lead content in powdered infant formula by means of quadrupole inductively coupled plasma mass spectrometry. Food Control 44:159–165
15. Feist B, Mikula B (2014) Preconcentration of heavy metals on activated carbon and their determination in fruits by inductively coupled plasma optical emission spectrometry. Food Chem 147: 302–306
16. Pushie MJ, Pickering IJ, Korbas M, Hackett MJ, George GN (2014) Elemental and chemically specific X-ray fluorescence imaging of biological systems. Chem Rev 114:8499–8541
17. Beltran B, Leal LO, Ferrer L, Cerda V (2015) Determination of lead by atomic fluorescence spectrometry using an automated extraction/pre-concentration flow system. J Anal Atom Spectrom 30:1072–1079
18. Li XY, Wu ZT, Zhou XD, Hu JM (2017) Colorimetric response of peptide modified gold nanoparticles: an original assay for ultrasensitive silver detection. Biosens Bioelectron 92:496–501
19. Xiao Y, Rowe AA, Plaxco KW, Heeger AJ (2007) Electrochemical detection of parts per billion lead via an electrode-bound DNAzyme assembly. Abstr Pap Am Chem S 233:449–449
20. Chung CH, Kim JH, Jung J, Chung BH (2013) Nuclease-resistant DNA aptamer on gold nanoparticles for the simultaneous detection of Pb2+ and Hg2+ in human serum. Biosens Bioelectron 41:827–832
21. Long F, Zhu A, Wang HC (2014) Optofluidics-based DNA structure-competitive aptasensor for rapid on-site detection of lead(II) in an aquatic environment. Anal Chim Acta 849:43–49
22. Rance GA, Marsh DH, Nicholas RJ, Khlobystov AN (2010) UV-vis absorption spectroscopy of carbon nanotubes: relationship between the pi-electron plasmon and nanotube diameter. Chem PhysLett 493:19–23
23. Bao Q, Zhang H, Yang JX, Wang S, Tang DY, Jose R, Ramakrishna S, Lim CT, Loh KP (2010) Graphene–polymer nanofiber membrane for ultrafast photonics. Adv Funct Mater 20:782–791
24. Guo S, Lin J, Penchev M, Yangel E, Ozkan M, Ozkan CS (2011) Label free DNA detection using large area Graphene-based FET biosensors. J Nanosci Nanotechno 11:5258–5263
25. Takeshima T, Sun L, Wang Y, Yamada Y, Nishi N, Yonezawa T, Fugetsu B (2014) Salmon milt DNA as a template for the mass production of Ag nanoparticles. Polym J 46:36
26. Jorio A, Fantini C, Dantas MSS, Pimenta MA, Souza AG, Samsonidze GG, Brar VW, Dresselhaus G, Dresselhaus MS, Swan AK, Unlu MS, Goldberg BB, Saito R (2002) Linewidth of the Raman features of individual single-wall carbon nanotubes. Phys Rev B 66(11):1–8
27. Byon HR, Choi HC (2006) Network single-walled carbon nanotube-field effect transistors (SWNT-FETs) with increased Schottky contact area for highly sensitive biosensor applications. J Am Chem Soc 128:2188–2189
28. Jiokeng SLZ, Dongmo LM, Ymele E, Ngameni E, Tonle IK (2017) Sensitive stripping voltammetry detection of Pb(II) at a glassy carbon electrode modified with an amino-functionalized attapulgite. Sensor Actuat B-Chem 242:1027–1034
29. Zidarič T, Jovanovski V, Menart E, Zorko M, Kolar M, Veber M, Hočevar S (2017) Multi-pulse galvanostatic preparation of nanostructured bismuth film electrode for trace metal detection. Sensor Actuat B-Chem 245:720–725
30. Xing H, Xu J, Zhu X, Duan X, Lu L, Wang W, Zhang Y, Yang T (2016) Highly sensitive simultaneous determination of cadmium (II), lead (II), copper (II), and mercury (II) ions on N-doped graphene modified electrode. Electroanal Chem 760:52–58
31. Taghdisi SM, Danesh NM, Lavaee P, Ramezani M, Abnous K (2016) An electrochemical aptasensor based on gold nanoparticles, thionine and hairpin structure of complementary strand of aptamer for ultrasensitive detection of lead. Sensor Actuat B-Chem 234: 462–469
32. Zhou Y, Tang L, Zeng G, Zhang C, Xie X, Liu Y, Wang J, Tang J, Zhang Y, Deng Y (2016) Label free detection of lead using impedimetric sensor based on ordered mesoporous carbon–gold nanoparticles and DNAzyme catalytic beacons. Talanta 146:641–647
33. Wang C, Cui X, Li Y, Li H, Huang L, Bi J, Luo J, Ma LQ, Zhou W, Cao Y (2016) A label-free and portable graphene FET aptasensor for children blood lead detection. Sci Rep 6:21711
34. Kanyong P, Rawlinson S, Davis J (2016) Gold nanoparticle modified screen-printed carbon arrays for the simultaneous electrochemical analysis of lead and copper in tap water. Microchim Acta 183: 2361–2368
35. Wang H, Zhao G, Zhang Z, Yi Y, Wang Z, Liu G (2017) A portable electrochemical workstation using disposable screen-printed carbon electrode decorated with multiwall carbon nanotube-ionic liquid and bismuth film for Cd (II) and Pb (II) determination. Int. J Electrochem Sci 12:4702–4713